Original Research

MicroRNA-34a alleviates steroid-induced avascular necrosis of femoral head by targeting *Tgif2* through OPG/RANK/RANKL signaling pathway

Wu-Xun Peng, Chuan Ye, Wen-Tao Dong, Lei-Luo Yang, Chun-Qing Wang, Ze-An Wei, Jian-Hua Wu, Qing Li, Jin Deng and Jian Zhang

Department of Orthopedics, The Affiliated Hospital of Guizhou Medical University, GuiYang 550004, P.R. China
Corresponding author: Jian Zhang. Email: zhangjianzj24@163.com

Impact statement

miR-34a can alleviate SANFH through targeting *Tgif2* and further regulating OPG/RANK/RANKL signaling pathway, which can be used as a new theoretical basis for SANFH treatment.

Abstract

The study aims to investigate the effect of microRNA-34a (miR-34a) targeting Tgif2 on steroid-induced avascular necrosis of femoral head (SANFH) by regulating OPG/RANK/RANKL signaling pathway. SD rats were divided into normal control and model (RNAKL rat models) groups. The model group was further assigned into model control, negative control, miR-34a mimics and miR-34a inhibitors groups. QRT-PCR was applied to detect miR-34a, Tgif2, OPG, RANK and RNAKL mRNA expressions. Femoral head tissues were collected for Micro-CT scanning and HE staining. QRT-PCR and Western blotting were used to detect expressions of miR-34a, Tgif2, OPG, RANK, RANKL and Runx2, OPN and OC in bone tissues. Dual-luciferase reporter gene assay was used to testify the target relationship between miR-34a and Tgif2. Compared with the normal control group, the model group showed increased Tgif2, RANK and RANKL mRNA expressions, but decreased miR-34a and OPG mRNA expressions. Tgif2 mRNA expression was negatively correlated with miR-34a and OPG mRNA expressions. Micro-CT showed cystic degeneration of femoral head, with decreased bone volume/total volume (BV/TV), bone surface area/bone volume and trabecular number in the model control group compared with the normal control group. Compared with the model control group, the miR-34a mimics group showed increased BV/TV and trabecular thickness and Runx2, OPN and OC expressions, while the parameters decreased in the miR-34a inhibitors group. Compared with the normal control group, the other groups showed increased Tgif2, RANK and RANKL expressions but decreased miR-34a and OPG expressions. Compared with the model control group, Tgif2, RANK and RANKL expressions decreased and miR-34a and OPG expressions increased in the miR-34a mimics group, while the miR-34a inhibitors group had a reverse trend in contrast to the miR-34a mimics group. Tgif2 is a target gene of miR-34a. In conclusion, miR-34a can alleviate SANFH through targeting *Tgif2* and further regulating OPG/RANK/RANKL signaling pathway.

Keywords: MiR-34a, steroid-induced avascular necrosis of femoral head, osteoprotegerin, receptor activator of nuclear factor Kappa B, receptor activator of nuclear factor Kappa ligand, signaling pathway

***Experimental Biology and Medicine* 2017; 242: 1234–1243. DOI: 10.1177/1535370217703975**

Introduction

Steroid-induced avascular necrosis of the femoral head (SANFH), a common nontraumatic osteonecrosis,[1] mainly includes necrosis of bone trabecula or marrow induced by a long-term history of using glucocorticoid.[2] Clinically, SANFH is characterized by hip discomfort, pain, activity limitation, limp and shortening of lower limbs.[3] Already proposed direct and indirect pathological mechanisms include apoptosis, inhibit formation of osteoblast and their precursors, vascular endothelial dysfunction, enhanced activity of coagulation, enhance production of ROS, inhibition of angiogenesis and increase adipocytes.[4] Various therapeutic procedures have been implemented; however, most of which did not show satisfactory clinical outcomes. Discovery of physiological bone metabolism parameters such as Receptor Activator of Nuclear factor Kappa B (RANK), Receptor Activator of Nuclear factor Kappa Ligand (RANKL) and Osteoprotegerin (OPG) and studies on physiologicaland pathological mechanisms of those provide new targets for the treatment of SANFH.[5,6]

Moreover, microRNA is essential in the formation of bone, indicating that microRNA might be a novel target for skeletal diseases' treatment.[7]

MiR-34a can inhibit tumor by participating in proliferation, migration and metastasis of tumor cells. In addition, evidence showed that miR-34a can suppress invasion and metastasis by directly regulating *Tgif2* in gastric cancer.[8] As a critical suppressor of osteoclastogenesis, miR-34a regulates bone resorption and the bone metastatic niche by targeting *Tgif2*, whose deletion may abolish miR-34a regulation.[9,10] In addition, *Tgif2* and RNAKL pathway forms a positive feedback loop: transcription factor induced by RNAKL pathway can enhance activity of *Tgif2* and *Tgif2* can promote the activity of transduction factor in RNAKL pathway so as to accelerate growth and differentiation of osteoclast.[9] Moreover, previous studies found that OPG, RANK and RNAKL signal pathway plays a vital role in the bone remodeling, among which RANK-RANKL interactions would increase osteoclast proliferation, enhance the activity and viability of osteoclast while OPG, a nature decoy receptor, can suppress the function of RANKL.[11,12] Interestingly, miR-34a is capable of regulating differentiation from rats' bone marrow stromal cells and from human's peripheral mononuclear cell to osteoclast; [9] therefore, we hypothesizes that miR-34a plays a vital role in SANFH. The present study explored the effects of miR-34a on OPG/RANK/RANKL signal pathway in SANFH using a rat model.

Materials and methods

Ethical statement

Current study was conducted with the approval of the Animal Experimentation Ethics Committee of The Affiliated Hospital of Guizhou Medical University. All efforts were made to minimum the suffering for animals

Animals

A total of 74 Sprague–Dawley (SD) male rats (12-week-old; 280–320 g) were provided by the Hunan SJA Laboratory Animal Co., Ltd (Hunan, China). All SD rats were group-housed (two rats/cage), with unlimited access to sterilized food and water in a standard diet. The cages were kept at 22–26°C and 37%–42% humidity on a reverse 12-h light/dark cycle.

Establishment of SANFH animal models

A total of 16 rats were randomly grouped into the Normal group. Then left 58 rats were used for the establishment of SANFH animal models. After feeding for one week, model rats were weighed and intraperitoneally injected with the lipopolysaccharide (LPS, Escherichia coli 055:B5, Sigma, USA), twice at 24-h intervals with 20 μg/kg each time; 24 h after the injection of the LPS, the rats were intramuscularly injected with methylprednisolone Sodium Succinate (40 mg/kg, Pfizer Pharmaceutical, China) for three times at a 24-h interval. Rats from normal group were intramuscularly injected with normal saline (40 mg/kg), three times at 24 h intervals each time. Six weeks after the final injection, two rats were selected randomly in both normal group and model group, and intraperitoneally injected with 10% hydrated acid. After anesthesia, bilateral femurs were harvested for the histomorphology test to verify whether the model construction is successful.

Animal grouping

Rats in model group were assigned into model control group, negative control group, miR-34a mimics group and miR-34a inhibitors group randomly (14 rats/group). Rats in the flur groups received 40 ul normal saline, 40 ul Negative control (5′-UUCUCCGAACGUGUCACGUTT-3′), 40 ul miR-34a mimics (5′-UGAGAUGAAGCACUGUAGC UC-3′) and 40 ul miR-34a inhibitors (5′- GAGCUACAGUG CUUCAUCUCA-3′) (Sagan Biotech Co., Ltd., Shanghai, China) by intra-bone marrow injection, separately. After being fed for four weeks, rats were sacrificed randomly. The bilateral femoral head samples were collected and embedded in 10% paraffin.

Sample collection

Based on rats' weight, they were intraperitoneally injected with 10% hydrated acid (4 ml/kg). After being successfully narcotized, rats were open cut along their abdominal cavity, and then their veins exposed; 7–8 ml blood sample was taken in tubes with heparin, centrifuged for 15 min at 3000 r/min. Then the upper serum (erythrocyte were excluded) was collected and stored at −20°C by classification. After that, rat's abdomen was exposed and their lower limbs were cut off to separate the soft tissue along the femur, followed by opening the joint capsule. After that, with greater trochanter as incision, ligaments and tissue around femoral head was detached from outside to inside, from downside to upside, and then rongeur was used to sever femoral head at the neck of femur to take out bilateral femurs. Then the bilateral femurs of all rats were placed into foam box with liquid nitrogen and then were assigned into two parts: the first part was placed in a −80°C cryogenic freezer, and the other part was embedded in paraffin.

Micro-CT scan

The micro-CT diagnosis is finished by Institute of Laboratory Animal Science, Chinese. The scanning was performed by Inveon micro PET/CT manufactured by Siemens (Berlin, Germany; 60 kV, 400 uA). Samples (31.25 μm thick) were scanned in a spatial resolution of 10 μm. Inveon analysis workstation was applied for 3D reconstruction analysis. The micro CT scan was performed on a 5 cm proximal end of the femurs. After that, the Bone volume/Total volume (BV/TV), Bone surface area/Bone volume (BS/BV), Trabecular thickness (Tb.Th) and Trabecular number (Tb.N) were computed by the workstation.

Hematoxylin-eosin (HE) staining

Rats' fresh femoral heads were taken and open cut along coronal plane. The femur specimens were firstly fixed in 4% poly formaldehyde for 36 h and then transferred into

solution with 4% paraformaldehyde ethylenediaminetetraacetic acid (EDTA). Two months later, samples were cut into about pieces of 1.0 cm^3 when there is no resistance for a pin to stab into femoral head. After decalcification, the tissues were dehydrated in graded ethanol and cleared in xylene, followed by being embedded in paraffin and cut into sections (4 μm thick). The sections went dewaxed with xylene, dehydrated by gradient ethanol and stained by hematoxylin for 5 min. Slides were washed briefly in distilled water at 40°C for 10 s, differentiated in HCl-ethanol for 30 s, stained by eosin for 2 min, dehydrated by gradient alcohol and transparentized by xylene. Afterwards, neutral balsam was used to mount the samples. The histopathological changes were observed under an optical microscope at ×200 magnifications.

Quantitative reverse transcription-polymerase chain reaction (qRT-PCR)

Total RNA was extracted using Trizol one-step method (Thermo Fisher Scientific Inc., USA). The RNA was dissolved by ultrapure water with diethylpyrocarbonate (DEPC). Subsequently, the concentration and purity of the RNA were confirmed by measuring absorbance at 260 nm and 280 nm with ND-1000 UV/VIS spectrometer (Nanodrop, USA). The RNA was reversed transcribed according to mammal cDNA synthesis kit (Fermentas, USA), and the reaction conditions were the following: 70°C for 10 min, ice bath for 2 min, 42°C for 60 min and 70°C for 10 min. The cDNA was stored at −80°C before use. qRT-PCR was performed to detect the samples' mRNA expressions of Runx2, OPN (Osteopontin), OC (Osteocalcin), Tgif2 and osteoprotegerin osteoclast differentiation factor/receptor Activator of NF-Kappa B/ receptor of activator of NF KB ligand (OPG/RANK/RANKL), and qRT-PCR mixture was purchased from Thermo Fisher Scientific Inc (Table 1). miR-34a reaction conditions were as follow: 40 cycles: 95°C pre-denaturation for 30 s, 95°C denaturation for 10 s and 60°C annealing for 20 s, then 72°C extension for 10 s. Other mRNA reaction condition was as follow: 40 cycles: 95°C pre-denaturation for 30 s, 95°C denaturation for 10 s and 60°C annealing for 20 s, then 72°C extension for 30 s. Specificity of amplified reaction was detected and analyzed by solubility curve. qRT-PCR was performed with iQ5, Bio-Rad, USA. The expression of miR-34a was normalized with U6 as internal reference, and in case of expressions of other target genes, β-actin acted as internal reference. All data were calculated using the comparative CT (ΔΔCT) method, and the equation $2^{-\Delta\Delta Ct}$ was adopted to calculate relative expressions of target genes. Each specimen would be repeated for three times.

Western blotting

The femoral heads were lysed in RIPA buffer and then centrifuged for 30 min at 12,000 r/min at 4°C. The supernatant, which is the extracted total cellular protein, was collected and added with 1×SDS (sodium dodecyl sulfate, sodium salt) loading buffer; 20 μl supernatant was taken and electrophoresed by 12% SDS–PAGE, then transferred onto a polyvinylidene fluoride membrane and blocked with PBS-T with 5% BSA at room-temperature for 1 h. The sealed liquid was washed, and membrane was placed into a plastic groove; 5% BSA was added to prepare corresponding concentrations of Runx2, OPN, OC, Tgif2, OPG, RANK, RANKL and β-actin antibodies (Cell Signaling Technology, Inc., USA) at 4°C overnight. On the next day, membranes were then washed with TBST (10 min × 3 times) and incubated with the second antibody (Abcam plc., UK) at 4°C for 4–6 h. After incubation, the membranes were washed with TBST (15 min × 3 times) and then developed by the horseradish peroxidase ECL equipment (solution A and B were mixed at 1: 1 by V/V). After development, all the Western blotting bands were analyzed for their relative optical density.

Table 1 Primers used for quantitative RT-PCR

Target gene	Primer sequence
miR-34a	Forward 5′-ATACCGCTCGAGCCTCCTGCA TCCTTTCTTT-3′
	Reverse 5′-ATACCGCTCGAGCCTGTGCC TTTTTCCTTCC-3′
U6	Forward 5′CTCGCTTCGGCAGCACATATACT3′
	Reverse 5′ACGCTTCACGAATTTGCGTGTC3 ′
Tgif2	Forward 5′-TAGGTACCCAGAAGCAGCAGGACCCA-3′
	Reverse 5′-GCAGATCTTCATCACTGAGCGGAGGC-3′
OPG	Forward 5′-TTGCACCACTCCAAATCCAG-3
	Reverse 5′-AATCGCACCCACAACCG-3′
RANK	Forward 5′-GTCTCATCGTCCTGCTCCTCTT-3′
	Reverse 5′-CAGCGTTTTCCCTCCCTTC-3′
RANKL	Forward 5′-GCATCGCTCTGTTCCTGTACTTT-3′
	Reverse 5′-GCTTCTGTGTCTTCGCTCTCC-3′
Runx2	Forward 5′-CCGGTCTCCTTCCAGGAT-3′
	Reverse 5′-GGGAACTGCTGTGGCTTC-3′
OPN	Forward 5′-CCTCCCGGTGAAAGTGAC-3′
	Reverse 5′-CTGTGGCGCAAGGAGATT-3′
OC	Forward 5′-CCTTCATGTCCAAGCAGGA-3′
	Reverse 5′-GGCGGTCTTCAAGCCATAC-3′
β-actin	Forward CGACCACACACAGAAGGAGAT
	Reverse GCCGATTCACACCGAGTA

RT-PCR: reversed transcription polymerase chain reaction; miR-34a: miRNA-34a; Tgif2: thymic stromal lymphopoietin; OPG: osteoprotegerin; RANK: receptor activator of NF-Kappa B; RANKL: receptor of activator of NF KB ligand; OPN: osteopontin; OC: osteoclasts.

Dual-luciferase reporter gene assay

The online miRNA target predication platform Targetscan (http://www.targetscan.org/) was used to screen the target gene of miR-34a, and to predict the 3′-UTR binding site of miR-34a and Tgif2. On the basis of the predicted binding site, Tgif2's 3′-UTR promoter sequence containing miR-34a binding site was synthesized and pGL-control carrier (Promega (Beijing) Biotech Co., Ltd., USA), *Kpn*I site and *Bgl*II site were inserted. 3′-UTR wild plasmid of Tgif2 was contracted and named pGL3-Tgif2-WT. Meanwhile, 3′-UTR

mutation plasmid of Tgif2 with miR-34a mutated binding site was constructed.

HEK293 cells in good condition was cultured and inoculated into 24-well plate (1×10^6 cells per well). In each well, 500 μL absolute RPMI 1640 substrate was added and them the plate was placed back into the incubator. The cells were cultured in a 37°C, 5% CO_2 incubator. When cells grew into the concentration of 85%, transfection was conducted with Lipofectamine 2000 (Sigma-Aldrich Co. LLC., USA), and all the operations were in strict accordance with construction of the reagent kit. In term of the transfection, four groups were divided: cells were transfected with respectively pGL3-Tgif2-WT and miR-34a mimics, pGL3-Tgif2-WT and miR-34a negative control, pGL3-Tgif2-MUT and miR-34a mimics and pGL3-Tgif2-MUT and miR-34a negative control. In each group, there was pGL3-Tgif2-WT/pGL3-Tgif2-MUT (100 ng), miR-34a mimics (50 ng) and miR-34a negative control (50 ng); 24 h after the transfection, cells were taken out of the incubator and rinsed with PBS. Then 100 μL cell lysis buffer (Beyotime Biotechnology Institution, Shanghai, China) was added into each well, and the plate was shaken until cells were fully disassociated. And at that time, the cell lysis buffer was transferred into 1.5 mL centrifuge tube to centrifuge the cells at 12000 r/min for 20 min. After that, the supernatant was taken to testify the relative activity of luciferase using Dual-luciferase kit. And the above experiment was repeated for three times.

Statistical analysis

The statistical analyses were conducted with SPSS 21.0(IBM SPSS Statistics, IBM Corporation). All experiments were calculated by means ± standard deviations. Multiple sets of data were analyzed using One-way ANOVA. Differences between groups were analyzed using *t*-test. Correlation between the parameter was performed by Pearson correlation analysis. Statistical significance was set when P value was less than 0.05.

Results

Model establishment and sample handling

In the molding process, rats in normal group had suitable hair, healthy body, frequent eating and drinking behavior, good state of mind and sensitive reaction; When being caught, they were alive without abnormal urinary and bowel elimination and with smooth articular surface of femoral head, clean cartilage, strong, hard and elastic bone. However, rats in the model group are gradually lighter were thinner with thinner subcutaneous fat layer; the water and food intake also decreased dramatically; the coat color was dark and mess, accompanied by increased hair removal; rats became pathetic and easily frightened; hind limbs were weak and some rats showed slight limp; stools were dry or loose; the cartilage was dark without gloss; bone was fragile and prone to divorced from surrounding tissue.

The condition of femoral head of rats in the normal and model groups

The micro-CT results showed that the normal shape of the bilateral femoral was observed in normal group and cartilage surface was smooth and thick, while the trabecular bone arranged regularly and compactly. On the contrary, in model group, there were irregular shape of the bilateral femoral head with necrosis and cystolization of the subchondral bone and sparse changes of trabecular bone. According to software quantitative analysis, Table 2 showed the parameter of trabecular in cancellous bone within the unit volume of the center of the femoral head. The BV/TV, BS/BV, and Tb.N in model group were significantly lower than those of in normal group (all $P < 0.05$), while no significant difference in Tb.Th was noticed between the two groups.

Pathologic morphology of rats in the normal and model groups

The femoral head was cut into slices and stained with hematoxylin-eosin (Figure 1). In the femoral head slices in normal group, there were smooth surface of cartilage, clear shape, even thickness, normal number, and rich blood vessels, rich hematopoietic cells in cancellous bone; besides, there were complete tidemarks, normal joint between calcification zone and bone trabecula with intact, regularly arranged, compacted and clear-structure bone trabecula; also, in bone cortex and trabecula, osteocyte was clearly seen with empty lacuna occasionally observed. In the slices of model group, cartilage became rough on its surface, thinner in its thickness, with parts of cartilage surface falling off, showing as uneven as steps. In bone trabecula, there were less hematopoietic cells, extended fat cells and disordered structure; besides, the discrete or even disappeared tidemarks were observed, and even, trabecula turned thinner, cracked or disappeared. In bone cortex and bone trabecula, there were a large number of osteocyte and bone matrix reduced or disappeared with a cloud of necrotic cells and more empty lacunas than normal group.

Table 2 Comparison of parameters of trabecular in the cancellous bone within the unit volume of the center of the femoral head between normal control group and model control group

Group	BV/TV	BS/BV	Tb.Th	Tb.N
Normal control group	0.72 ± 0.07	25.07 ± 2.52	0.14 ± 0.02	6.34 ± 0.63
model control group	0.59 ± 0.06[a]	21.25 ± 2.10[a]	0.13 ± 0.01	5.83 ± 0.58[a]

[a]Compared with the normal control group, $P < 0.05$; BV/TV, bone volume/total volume.
BS/BV: bone surface area/bone volume; Tb.Th: trabecular thickness; Tb.N: trabecular number.

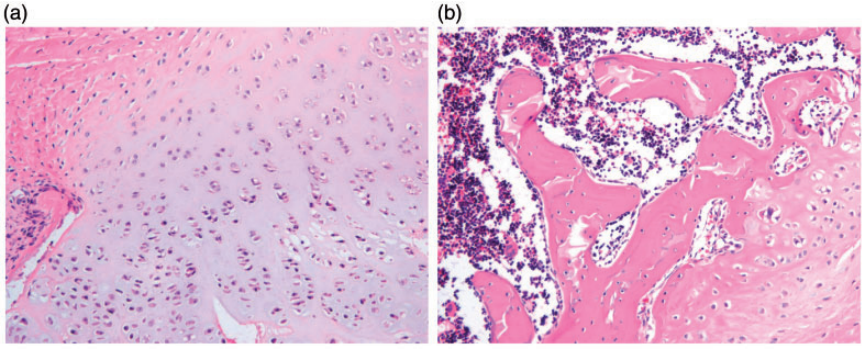

Figure 1 The morphology changes in the femoral head between normal control group and model control group (× 200). (a) normal control group; (b) model control group. (A color version of this figure is available in the online journal.)

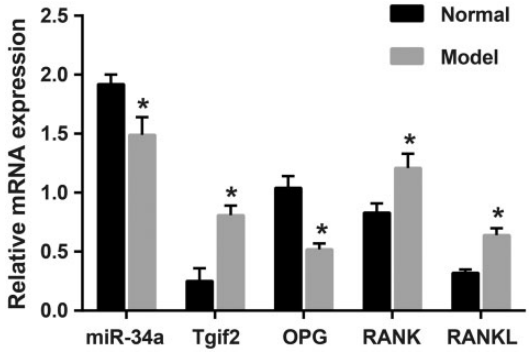

Figure 2 The expressions of miR-34a, *Tgif2* and OPG/RANK/RANKL mRNA among normal control and model control groups. Note: *compared with the normal control group, $P < 0.05$; Tgif2: thymic stromal lymphopoietin; OPG: osteoprotegerin; RANK: receptor activator of NF-Kappa B; RANKL: receptor of activator of NF KB ligand; miR-34a, miRNA-34a

The expressions of miR-34a, Tgif2, OPG, RANK and RANKL mRNA in the normal and model groups

Expressions of miR-34a, Tgif2 and OPG/RANK/RANKL mRNA in normal group and model group were shown in Figure 2. Compared to those in the normal group, *Tgif2*, RANK and RANKL mRNA expressions in the Model group were significantly increased, while miR-34a and OPG mRNA expressions were significantly decreased ($P < 0.05$). After analysis by the Pearson correlation, it was showed that miR-34a and *Tgif2* mRNA expressions were correlated negatively, r (Pearson correlation coefficient) = −0.685 ($P < 0.001$); miR-34a and OPG mRNA expressions assumed the intermediately positive correlation, r = 0.505 ($P < 0.001$); *Tgif2* mRNA expression was negatively correlated with OPG mRNA expression, r = 0.550 ($P < 0.001$); *Tgif2* mRNA expression was positively correlated to RANK mRNA expression moderately, r = 0.423 ($P < 0.001$); *Tgif2* and RANKL mRNA expression had a moderate positive correlation, r = 0.598 ($P < 0.001$).

BV/TV, BS/BV, Tb.Th and Tb.N among the normal control, model control, negative control, miR-34a mimics and miR-34a inhibitor groups

By the standard of micro CT, normal group shows even cartilage surface and that trabecular bone arranged regularly and compactly. In model control group, irregular shape of the bilateral femoral head, sparse trabecular bone, and thinner cartilage surface was shown. In model control group, femoral head was flat in company with cystic degeneration and parentally sparse trabecular bone. miR-34a mimics group showed normal shape of femoral head, dense trabecular bone without obvious cystic change. Results of negative control group were between those of mimics and inhibitors group, similar to those of the model group. Software was used to quantify parameters of trabecular in the cancellous bone within the unit volume of the center of the femoral head (Table 3). Compared to normal group, the other groups markedly had lower BV/TV, BS/BV and Tb.N ($P < 0.05$). Compared to model group, miR-34a inhibitors group had a remarkable decrease in BV/TV, BS/BV and Tb.N, while miR-34a mimics group showed a remarkable increase in all parameters. There are no differences between negative control group and model control group. No significant difference in Tb.Th among the five groups was identified (all $P > 0.05$).

Morphology changes among the normal control, model control, negative control, miR-34a mimics and miR-34a inhibitor groups

The femoral head of rats in each group was stained with hematoxylin-eosin (Figure 3). In normal control group, the articular cartilage surface was found to be smooth and clean, articular cartilage matrix was rich and the number of isogenous chondrocytes was normal. The bone trabeculae were regularly arranged, with complete structure, clearly visible osteocytes and a few empty lacunaes. In the femoral head slices in model control group, the osseous trabecular was scattered or even fractured with disordered structure and fragmentation. Furthermore, the number of empty bone lacunae notably increased; spots-like necrosis of bone marrow and fibrous hyperplasia appeared. In the negative control group, the number of isogenous chondrocyte and articular cartilage matrix was decreased. The osseous trabecular was broken and a lot of empty lacunae were found. In the miR-34a inhibitors group slices, necrosis of cartilage cells was serious with heavy stain; arthrodial cartilage injury was severe and there were lots of necrotic material; tidal

Table 3 Comparison of parameters of trabecular in the cancellous bone within the unit volume of the center of the femoral head among normal control, model control, negative control, miR-34a mimics and miR-34a inhibitor groups

Group	BV/TV	BS/BV	Tb.Th	Tb.N
Normal control	0.71 ± 0.07	24.92 ± 2.51	0.14 ± 0.03	7.02 ± 0.69
Model control	0.55 ± 0.05^{a}	20.13 ± 2.01^{a}	0.13 ± 0.02	5.65 ± 0.56^{a}
Negative control	0.52 ± 0.05^{a}	20.07 ± 2.00^{a}	0.13 ± 0.02	5.63 ± 0.56^{a}
miR-34a inhibitor	$0.46 \pm 0.04^{a,b}$	$17.75 \pm 1.75^{a,b}$	0.15 ± 0.04	$5.00 \pm 0.51^{a,b}$
miR-34a mimics	$0.63 \pm 0.06^{a,b}$	$22.39 \pm 2.22^{a,b}$	0.14 ± 0.02	$6.39 \pm 0.63^{a,b}$

[a]Compared to normal control group, $P < 0.05$.
[b]Compared to model control group, $P < 0.05$.
BV/TV: bone volume/total volume; BS/BV: bone surface area/bone volume; Tb.Th: trabecular thickness; Tb.N: trabecular number.

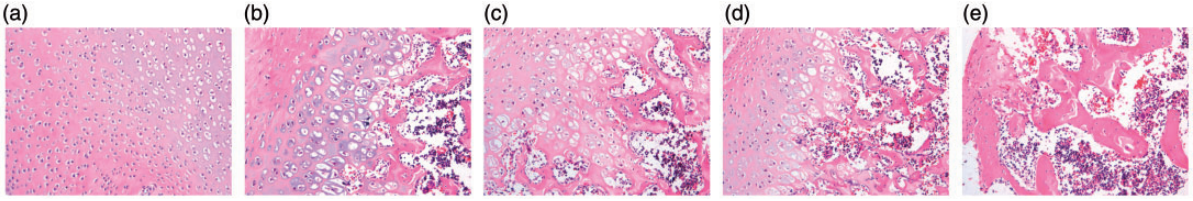

Figure 3 Comparison of the morphology changes in the femoral head by HE staining among (×100) among normal control, model control, negative control, miR-34a mimics and miR-34a inhibitor groups. (a), normal control group; (b), model control group; (c), negative control group; (d), miR-34a mimics group; (e), miR-34a inhibitors group; miR-34a, miRNA-34a. (A color version of this figure is available in the online journal.)

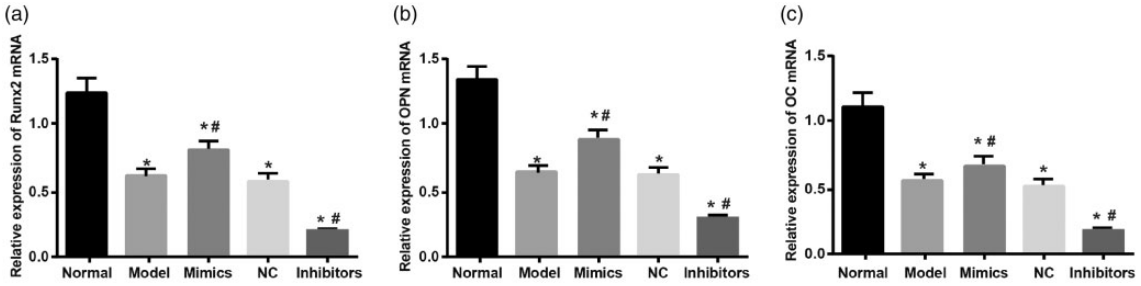

Figure 4 Comparison of expressions of Runx2, OPN and OC mRNA among normal control, model control, negative control, miR-34a mimics and miR-34a inhibitor groups. (a) comparison of expression of Runx2; (b) comparison of expression of OPN; (c) comparison of expression of OC; *compared with the normal control group, $P < 0.05$; #compared with model control group and negative control group, $P < 0.05$; OPN: osteopontin; OC: osteoclasts; miR-34a: miRNA-34a

line was broken even disappeared; the osseous trabecular became broken and vanished; bone matrix was badly damaged and osteonecrosis of femoral head was exist. In the femoral head slices of miR-34a mimics group, articular cartilage matrix was low with uneven distributed red presenting; isogenous chondrocytes declined; mounts of bone-like dense connective tissue began to hyperplasia; be rich in vascular or venous sinus with hyperemia; hematopoietic tissue in marrow cavity was less accompanied by lipocytes; the bony trabeculae was sparse and some of them were fractured.

The expressions of Runx2, OPN and OC mRNA and protein in rat models among the normal control, model control, negative control, miR-34a mimics and miR-34a inhibitor groups

According to RT-PCR and western blotting (Figures 4 and 5), compared to normal control group, other groups (model control, negative control, miR-34a mimics and miR-34a inhibitor) showed decreased expressions of Runx2, OPN and OC mRNA and protein ($P < 0.05$). In model group, there was no difference in the expressions of above factors between negative control and model control groups (all $P > 0.05$). In comparison of model control and negative control groups, miR-34a mimics group had increased expressions of Runx2, OPN and OC mRNA; miR-34a, whereas inhibitors group exhibited remarkably decreased expressions of Runx2, OPN and OC mRNA and protein (all $P < 0.05$)

The expressions of miR-34a, Tgif2, OPG, RANK and RANKL mRNA in rats' bone tissue among the normal control, model control, negative control, miR-34a mimics and miR-34a inhibitor groups

Results of samples from each group detected by RT-PCR are presented in Figure 6. Compared to *Tgif2*, RANK

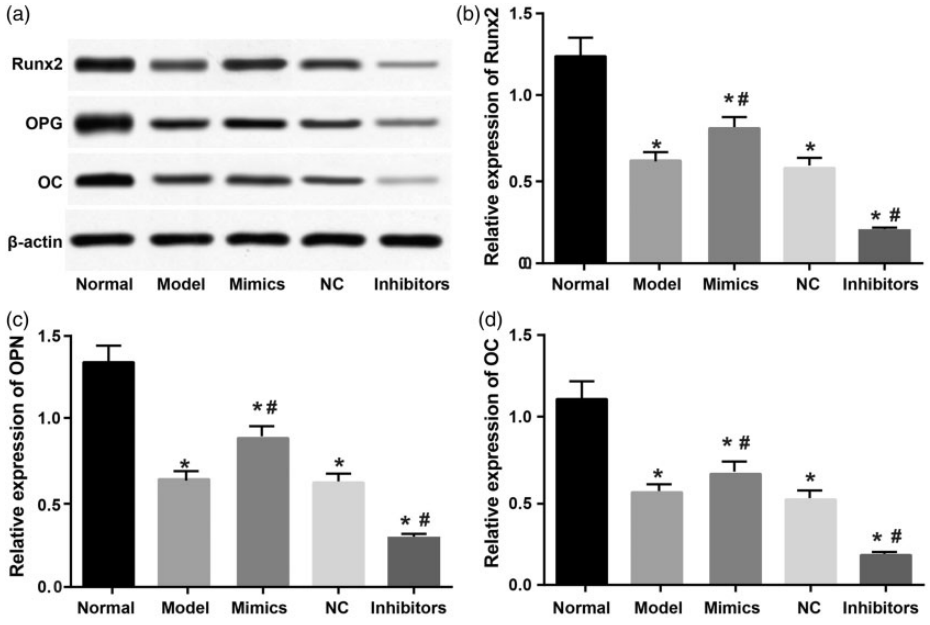

Figure 5 Comparison of expressions of Runx2, OPN and OC protein in bone tissues among normal control, model control, negative control, miR-34a mimics and miR-34a inhibitor groups.(a) comparison of expression of Runx2; (b) comparison of expression of OPN; (c) comparison of expression of OC; *compared with the normal control group, $P < 0.05$; #compared with model control group and negative control group, $P < 0.05$; OPN: osteopontin; OC: osteoclasts; miR-34a: miRNA-34a

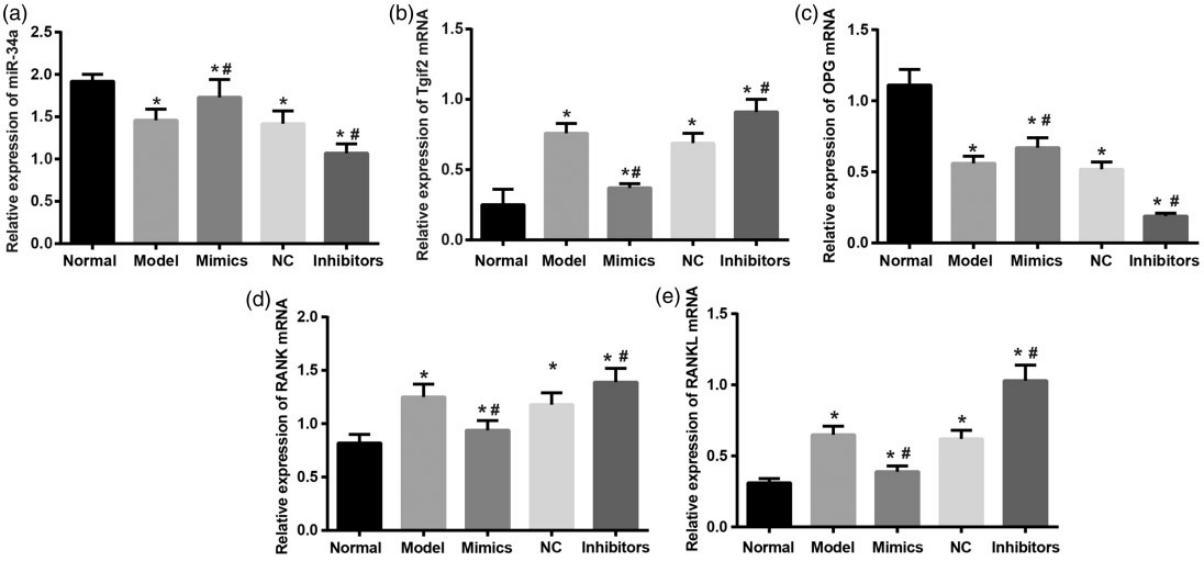

Figure 6 Comparison of expressions ofmiR-34a, Tgif2 and OPG/RANK/RANKL mRNA among normal control, model control, negative control, miR-34a mimics and miR-34a inhibitor groups. (a), expression of miR-34a; (b), expression of Tgif2; (c), expression of OPG; (d), expression of RANK; (e), expression of RANKL; *compared with the normal control group, $P < 0.05$; #compared with model control group and negative control group, $P < 0.05$; Tgif2: thymic stromal lymphopoietin; OPG: osteoprotegerin; RANK: receptor activator of NF-Kappa B; RANKL: receptor of activator of NF KB ligand; miR-34a: miRNA-34a

and RANKL mRNA expressions in the Normal group, those in the other groups were significantly increased; miR-34a and OPG mRNA expressions were obviously decreased (all $P < 0.05$). In model group, there was no significant difference in expressions of above factors mRNA between negative control and normal control groups (all $P > 0.05$). Compared to those in the model control group and negative control groups, expressions of miR-34a and OPG mRNA in miR-34a mimics group remarkably increased, while expressions of *Tgif2*, RANK and RANKL mRNA greatly decreased (all $P < 0.05$). In miR-34a inhibitors group, expressions of miR-34a and OPG mRNA were lower; however, expressions of *Tgif2*, RANK and RANKL mRNA were much higher (all $P < 0.05$). These results indicated that miR-34a may promote expression of OPG mRNA and inhibit expressions of RANK and RANKL mRNA by directly down-regulating *Tgif2*.

The expression of Tgif2, OPG, RANK and RANKL protein in rats' femoral head among the normal control, model control, negative control, miR-34a mimics and miR-34a inhibitor groups

Results of samples from each group were detected by Western blotting (Figure 7). Compared to the normal control group, the expression of OPG obviously decreased and expressions of Tgif2, RANK and RANKL protein significantly increased in the other groups (normal control, model control, negative control, miR-34a mimics and miR-34a inhibitor groups) (all $P < 0.05$). In model group, there was no significant difference in expressions of above factors protein between negative control group and model control group (all $P > 0.05$). Compared to model control group and negative control group, expressions of *Tgif2*, RANK and RANKL mRNA in miR-34a mimics group were greatly down-regulated, while expressions of OPG were markedly up-regulated (all $P < 0.05$). In miR-34a inhibitors group, expressions of Tgif2, RANK and RANKL protein were much higher; however, expression of OPG protein were significantly lower (all $P < 0.05$). These results indicate that miR-34a may promote OPG protein expression and inhibit RANK and RANKL protein expression by directly down-regulating Tgif2.

Target relationship between miR-34a and Tgif2

After prediction by online miRNAs target gene predicting platform Targetscan (http://www.targetscan.org/), it was found that *Tgif2* is one of the target gene of miR-34a, for there was a binding site of miR-34a and 3′-UTR of Tgif2 (Figure 8(a)). According to the result of dual-luciferase reporter assay, transfection of pGL3-Tgif2-WT and miR-34a mimics caused lower activity in comparison with miR-34a NC group ($P < 0.05$). However, relative luciferase activity change was seen after transfection of pGL3-Tgif2-MUT between miR-34a mimics and miR-34a NC groups (Figure 8(b)). The result was in accordance with prediction on bioinformatics, which further confirmed that miR-34a could bind to base in 3′-UTR area of Tgif2, targeting Tgif2.

Discussion

SANFH is a common non-traumatic femoral head necrosis with difficult rehabilitation and poor prognosis, bringing about serious threat to the health and quality of life of patients.[6] A study reported mechanism of miR-34a in osteoporosis and found that miR-34a can affect growth and differentiation of osteoclast and osteoblast by mediating several signal pathways.[13] Therefore, insights into the effects and mechanisms of miR-34a's regulation on OPG/RANK/RANKL signal pathway by targeting *Tgif2* could offer new way to treat SANFH.

In the present study, compared to those in the normal control group, the mRNA and protein expression levels of *Tgif2*, RANK and RANKL were significantly increased, while the levels of miR-34a and OPG were greatly reduced in the other groups; reverse phenomenon was seen after miR-34a inhibitors interfering with models, implying that regulation pathways of these factors are related to pathological process of femoral head necrosis. OPG, an inhibitor of osteoclast paracrine, is produced by osteoblast. It combines with RANKL to reduce the combination between RANKL and RANK so as to suppress the activation of osteoclast.[14] Therefore, OPG expression is negatively correlated to RANKL and RANK expression. OPG/RANK/RANKL signaling pathway is vital in bone metabolism. RANKL combines with processors of osteoclast or RANK on its surface, enhances differentiation and activation of osteoclast, and inhibits its apoptosis. While OPG can effectively prevent RANKL and RANK interaction so as to inhibit

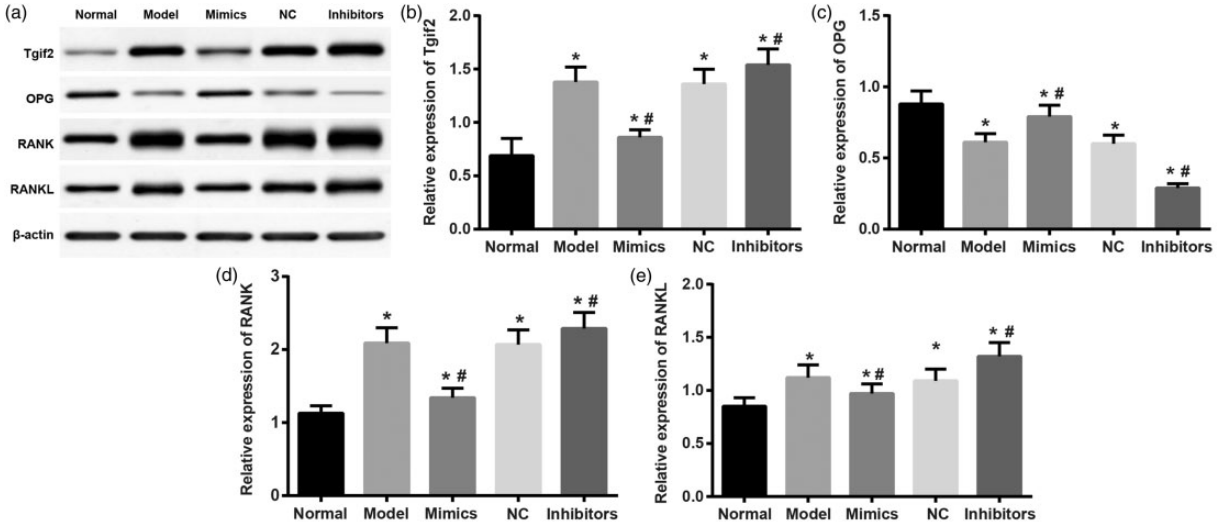

Figure 7 Comparisons of expressions of Tgif2, OPG, RANK and RANKL protein in bone tissues among normal control, model control, negative control, miR-34a mimics and miR-34a inhibitor groups. (a) Western blotting was performed to detect the expressions of Tgif2, OPG, RANK and RANKL; (b) expression of Tgif2; (c) expression of OPG; (d) expression of RANK; (e) expression of RANKL; *compared with the normal control group, $P < 0.05$; #compared with model control group and negative control group, $P < 0.05$; Tgif2: thymic stromal lymphopoietin; OPG: osteoprotegerin; RANK: receptor activator of NF-Kappa B; RANKL: receptor of activator of NF KB ligand; miR-34a: miRNA-34a

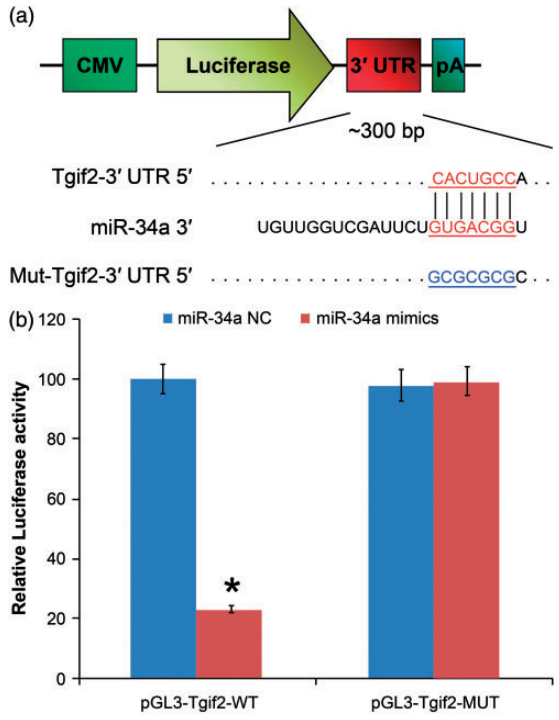

Figure 8 Target relationship between miR-34a and Tgif2 detected by dual-luciferase reporter gene assay. (a) The predicted binding site of miR-34a and 3′-UT of Tgif2 on Targetscan; (b) relative luciferase activity of miR-34a NC and miR-34a mimic; *compared with miR-34a NC group, $P < 0.05$; Tgif2: thymic stromal lymphopoietin; miR-34a: miRNA-34a. (A color version of this figure is available in the online journal.)

osteoclast differentiation and promote its apoptosis.[15,16] Similar studies found that miR-34c can directly target *Tgif2* gene and over expression of miR-34c leads to down-regulation of *Tgif2* after mRNA transcription and at protein translation level.[17] Tgif2 and RNAKL pathway forms a positive feedback loop: transcription factor induced by RNAKL pathway can enhance activity of *Tgif2* and *Tgif2* can promote the activity of transduction factor in RNAKL pathway so as to accelerate growth and differentiation of osteoclast.[8] Therefore, miR-34a can directly down regulate *Tgif2*, promote proliferation of osteoblast as well as inhibit transduction of OPG/RANK/RANKL signaling pathway.[8] On the other hand, some studies prove that OPG/RANK/RANKL signaling pathway takes part in the process of tumor occurrence and tissue specific metastasis in many kinds of cancer.[18,19] In malignant osteolytic lesion like multiple myeloma, abnormity in regulation of OPG/RANK/RANKL system or blocked formation of OPG makes OPG fail to counteract bone destruction resulted from up regulation of RANKL expression.[20] In addition, research confirmed that RNA interference blocks specific gene expression through mRNA analogs degradation performed by specific double strand RNA.[21] As a result, miR-34a inhibitors interfere with miR-34a expression, and its effect of regulation on *Tgif2* is decreased. So that *Tgif2* expression increases, which indirectly affect OPG/RANK/RANKL signaling pathway.

In addition, combined with Micro-CT analysis, we found that compared with that in model control group, rats in miR-34a mimics group showed much higher parameters such as BV/TV and Tb.Th, while rats in miR-34a inhibitors group showed much lower parameters. Reconstruction of bone means that the absorption and formation are always in homeostasis. If the process of bone-resorbing and bone-forming is out of balance, the mass and matrix of bones will become abnormal.[22] If the relative concentration between RANKL and OPG is unbalanced, activity of osteoclast will be enhanced, leading to osteoporosis.[23] According to some relative research, the ratio of OPG/RANKL is an early predictor of increase in bone absorption. So it might be an essential biomarker of bone injury.[24] Therefore, expression of miR-34a may regulate bone cells by downregulate *Tgif2* expression.

Apart from the relationship among miR-34a, Tgif2, OPG, RANK and RANKL, the study also indicates that compared to model control group, miR-34a mimics group had increased expression of Runx2, OPN and OC, while the miR-34a mimics group showed the opposite result. Runx2 is a multifunctional transcription factor capable of controlling skeletal development by mediating differentiation of osteoblasts and chondrocytes and expressions of many extracellular matrix proteins genes during the differentiation of chondrocyte and osteoblast.[25] In Fan *et al.*'s[26] study, it was showed that miR-34a could up-regulated the expression of RUNX2 by targeting NOTCH1, RBP2, and CYCLIN D1. OPNt is a prominent component of the mineralized extracellular matrix of bone,[27] and the balance of RANKL/RANK and OPG plays a vital role in isphysiological bone remodeling and osteoclastogenesis modulation.[28] As OPG is a competitive inhibitor of RANK binding to RANKL,[29] the decreased expression of RANK in mimic group may attribute to the increased OPG. In the case of OC, which is related to glucose metabolism, bone metabolism, and fat mass,[30] there is a study showing that knockdown of miR-34b/c enhanced OC mRNA expression;[31] however, the relation between miR-34a and remains unknown, which needs future exploration.

In conclusion, our study confirmed that expression of miR-34a can negatively targeting Tgif2 and may indirectly regulate OPG/RANK/RANKL signaling pathway so as to alleviate SANFH in rats. To better elucidate the mechanism involved, it is required that more well-designed studies are need in future.

Authors' contributions: WXP, WTD and ZAW designed the study. CY, JHW, QL, and JZ collated the data, designed and developed the database, carried out data analyses and produced the initial draft of the manuscript. LLY, CQW and JD contributed to drafting the manuscript. All authors have read and approved the final submitted manuscript.

ACKNOWLEDGMENTS

We would like to acknowledge the helpful comments on this article received from our reviewers. This study was supported by a grant from 2012 Annual Social Research Project of the Science and Technology Department of Guizhou Province (No: 2012-3125), Health Department Fund Project of Guizhou Province (No:gzwkj2012-1-023), the Key Applied Topic of Western Medicine Clinical of Guizhou Province Governor

Fund (No: 2012-127) and 2012 Affiliated Hospital of Guiyang Medical College Hospital Fund (NO:1-2012-10).

DECLARATION OF CONFLICTING INTERESTS

The author(s) declared no potential conflicts of interest with respect to the research, authorship, and/or publication of this article.

REFERENCES

1. Zhang C, Zou YL, Ma J, Dang XQ, Wang KZ. Apoptosis associated with wnt/beta-catenin pathway leads to steroid-induced avascular necrosis of femoral head. *BMC Musculoskelet Disord* 2015;**16**:132
2. Erken HY, Ofluoglu O, Aktas M, Topal C, Yildiz M. Effect of pentoxifylline on histopathological changes in steroid-induced osteonecrosis of femoral head: experimental study in chicken. *Int Orthop* 2012;**36**:1523–8
3. Kaushik AP, Das A, Cui Q. Osteonecrosis of the femoral head: an update in year 2012. *World J Orthop* 2012;**3**: 49–57
4. Lee YJ, Lee JS, Kang EH, Lee YK, Kim SY, Song YW, Koo KH. Vascular endothelial growth factor polymorphisms in patients with steroid-induced femoral head osteonecrosis. *J Orthop Res* 2012;**30**:21–7
5. Ney JT, Fehm T, Juhasz-Boess I, Solomayer EF. Rank, rankl and opg expression in breast cancer - influence on osseous metastasis. *Geburtshilfe Frauenheilkd* 2012;**72**:385–91
6. Song HM, Wei YC, Li N, Wu B, Xie N, Zhang KM, Wang SZ, Wang HM. Effects of wenyangbushen formula on the expression of vegf, opg, rank and rankl in rabbits with steroid-induced femoral head avascular necrosis. *Mol Med Rep* 2015;**12**:8155–61
7. Papaioannou G, Mirzamohammadi F, Kobayashi T. Micrornas involved in bone formation. *Cell Mol Life Sci* 2014;**71**:4747–61
8. Hu Y, Pu Q, Cui B, Lin J. Microrna-34a inhibits tumor invasion and metastasis in gastric cancer by targeting tgif2. *Int J Clin Exp Pathol* 2015;**8**:8921–8
9. Krzeszinski JY, Wei W, Huynh H, Jin Z, Wang X, Chang TC, Xie XJ, He L, Mangala LS, Lopez-Berestein G, Sood AK, Mendell JT, Wan Y. Mir-34a blocks osteoporosis and bone metastasis by inhibiting osteoclastogenesis and tgif2. *Nature* 2014;**512**:431–5
10. Wei J, Shi Y, Zheng L, Zhou B, Inose H, Wang J, Guo XE, Grosschedl R, Karsenty G. Mir-34s inhibit osteoblast proliferation and differentiation in the mouse by targeting satb2. *J Cell Biol* 2012;**197**:509–21
11. Hadjidakis DJ, Androulakis II. Bone remodeling. *Ann N Y Acad Sci* 2006;**1092**:385–96
12. Roshandel D, Holliday KL, Pye SR, Boonen S, Borghs H, Vanderschueren D, Huhtaniemi IT, Adams JE, Ward KA, Bartfai G, Casanueva F, Finn JD, Forti G, Giwercman A, Han TS, Kula K, Lean ME, Pendleton N, Punab M, Silman AJ, Wu FC, Thomson W, O'Neill TW, Group ES. Genetic variation in the rankl/rank/opg signaling pathway is associated with bone turnover and bone mineral density in men. *J Bone Miner Res* 2010;**25**:1830–8
13. Lopes HB, Ferraz EP, Almeida AL, Florio P, Gimenes R, Rosa AL, Beloti MM. Participation of microrna-34a and rankl on bone repair induced by poly(vinylidene-trifluoroethylene)/barium titanate membrane. *J Biomater Sci Polym Ed* 2016;**27**:1369–79
14. Martin TJ, Sims NA. Rankl/opg; critical role in bone physiology. *Rev Endocr Metab Disord* 2015;**16**:131–9
15. Tanaka S. Signaling axis in osteoclast biology and therapeutic targeting in the rankl/rank/opg system. *Am J Nephrol* 2007;**27**:466–78
16. Chen YC, Sosnoski DM, Mastro AM. Breast cancer metastasis to the bone: mechanisms of bone loss. *Breast Cancer Res* 2010;**12**:215
17. Wang Y, Wang CM, Jiang ZZ, Yu XJ, Fan CG, Xu FF, Zhang Q, Li LI, Li RF, Sun WS, Zhang ZH, Liu YG. Microrna-34c targets tgfb-induced factor homeobox 2, represses cell proliferation and induces apoptosis in hepatitis b virus-related hepatocellular carcinoma. *Oncol Lett* 2015;**10**:3095–102
18. Todenhofer T, Hennenlotter J, Schmiedel BJ, Hohneder A, Grimm S, Kuhs U, Salih HR, Buhring HJ, Fehm T, Gakis G, Blumenstock G, Aufderklamm S, Schilling D, Stenzl A, Schwentner C. Alterations of the rankl pathway in blood and bone marrow samples of prostate cancer patients without bone metastases. *Prostate* 2013;**73**:162–8
19. Santini D, Perrone G, Roato I, Godio L, Pantano F, Grasso D, Russo A, Vincenzi B, Fratto ME, Sabbatini R, Della Pepa C, Porta C, Del Conte A, Schiavon G, Berruti A, Tomasino RM, Papotti M, Papapietro N, Onetti Muda A, Denaro V, Tonini G. Expression pattern of receptor activator of nfkappab (rank) in a series of primary solid tumors and related bone metastases. *J Cell Physiol* 2011;**226**:780–4
20. Wittrant Y, Theoleyre S, Chipoy C, Padrines M, Blanchard F, Heymann D, Redini F. Rankl/rank/opg: New therapeutic targets in bone tumours and associated osteolysis. *Biochim Biophys Acta* 2004;**1704**:49–57
21. Tinoco ML, Dias BB, Dall'Astta RC, Pamphile JA, Aragao FJ. In vivo trans-specific gene silencing in fungal cells by in planta expression of a double-stranded rna. *BMC Biol* 2010;**8**:27
22. Bonjour JP. Calcium and phosphate: a duet of ions playing for bone health. *J Am Coll Nutr* 2011;**30**:438S–48
23. Lems WF. Fracture risk estimation may facilitate the treatment gap in osteoporosis. *Ann Rheum Dis* 2015;**74**:1943–5
24. Chmielnicka M, Wozniacka A, Torzecka JD. The influence of corticosteroid treatment on the opg/rank/rankl pathway and osteocalcin in patients with pemphigus. *Postepy Dermatol Alergol* 2014;**31**:281–8
25. Komori T. Regulation of bone development and extracellular matrix protein genes by RUNX2. *Cell Tissue Res* 2010;**339**:189–95
26. Fan C, Jia L, Zheng Y, Jin C, Liu Y, Liu H, Zhou Y. MiR-34a Promotes osteogenic differentiation of human adipose-derived stem cells via the RBP2/NOTCH1/CYCLIN D1 coregulatory network. *Stem Cell Rep* 2016;**7**:236–48
27. Saito K, Nakatomi M, Ida-Yonemochi H, Ohshima H. Osteopontin is essential for type I collagen secretion in reparative dentin. *J Dent Res* 2016;**95**:1034–41
28. Minenna G, D'Amore S, Maggiolini P, Scagliusi P, D'Amore M. [RANKL/RANK, OPG and OPT in a group of patients affected by chronic arthritis. *Preliminary report]*. Recenti Prog Med 2005;**96**:431–2
29. Chmielnicka M, Wozniacka A, Torzecka JD. The influence of corticosteroid treatment on the OPG/RANK/RANKL pathway and osteocalcin in patients with pemphigus. *Postepy Dermatol Alergol* 2014;**31**:281–8
30. Kanazawa I, Yamaguchi T, Yamamoto M, Yamauchi M, Kurioka S, Yano S, Sugimoto T. Serum osteocalcin level is associated with glucose metabolism and atherosclerosis parameters in type 2 diabetes mellitus. *J Clin Endocrinol Metab* 2009;**94**:45–9
31. Tamura M, Uyama M, Sugiyama Y, Sato M. Canonical Wnt signaling activates miR-34 expression during osteoblastic differentiation. *Mol Med Rep* 2013;**8**:1807–11

(Received August 2, 2016, Accepted March 11, 2017)